NASA Technical Memorandum 4199

Postbuckling Response of Long Thick Isotropic Plates Loaded in Compression Including Higher Order Transverse Shearing Effects

Manuel Stein and P. Daniel Sydow
Langley Research Center
Hampton, Virginia

Liviu Librescu
Virginia Polytechnic Institute and State University
Blacksburg, Virginia

National Aeronautics and
Space Administration
Office of Management
Scientific and Technical
Information Division

1990

Abstract

This paper presents buckling and postbuckling results for simply supported aluminum plates loaded in compression. Buckling results have been plotted to show the effects of thickness on the buckling stress coefficient. Buckling results are given for various length-to-width ratios. Postbuckling results for plates with transverse shearing flexibility are compared with results from classical theory for various width-to-thickness ratios. The plates are considered to be long with side edges simply supported and free of stress. The plates are subjected to a longitudinal compressive end-shortening displacement. Characteristic curves indicating the average longitudinal direct stress resultant as a function of the applied displacements are calculated based on four different theories: classical Von Karman theory, first-order shear deformation theory, higher order shear deformation theory, and three-dimensional flexibility theory. Present results indicate that the three-dimensional flexibility theory gives the lowest buckling loads and, therefore, the most accurate results. The higher order shear deformation theory has fewer unknowns than the three-dimensional flexibility theory but is not as accurate. The figures presented show that for postbuckling small differences occur in the average longitudinal direct stress resultant, in the maximum values of the transverse stress resultant and shear stress resultant, and in the maximum transverse displacements calculated when the effects of transverse shear flexibility are included in the various theories.

Introduction

The increasing interest in minimum weight designs for aeronautical and aerospace structures has generated substantial interest in the analysis of the elastic stability and postbuckling behavior of structures subjected to compressive in-plane loads. For thin homogeneous plates, classical plate theory predicts deformations and in-plane stresses that are comparable to those of three-dimensional elasticity. Transverse stresses in thin plates are generally small compared to in-plane stresses, and thus both classical theory and first-order shear deformation theory give satisfactory results. However, since both theories are two-dimensional, they are not accurate enough to predict transverse stresses directly. Accurate nonlinear theories are required for the analysis of thick plates, in which these transverse stresses become more significant.

It is often sufficient to use an accurate nonlinear two-dimensional theory to solve some three-dimensional nonlinear elasticity problems. One such theory has been derived in reference 1 for laminated and thick plates with three-dimensional flexibility effects. This theory can predict directly the transverse stresses as well as the in-plane stresses by using trigonometric terms in addition to the usual constant and linear terms representing through-the-thickness variation of the displacements. However, this theory cannot satisfy the surface boundary conditions of a plate.

The purpose of the present paper is to present the results of an investigation of the buckling and postbuckling response of isotropic plates loaded in compression using classical nonlinear Von Karman theory and three nonlinear transverse shearing theories and to compare results for these four theories for different values of plate width-to-thickness ratios in the postbuckling range. The nonlinear transverse shearing theories are first-order shear deformation theory (refs. 2 and 3), higher order shear deformation theory (ref. 4), and three-dimensional flexibility theory (ref. 1). The present derivation of the higher order shear deformation theory has the advantage of having nonlinear through-the-thickness terms without contributing additional unknowns to first-order shear deformation theory. In addition, it satisfies the surface boundary conditions of the plate. The essential difference between the theories is the use of cubic or trigonometric terms in addition to the constant and linear terms that represent the through-the-thickness variation of the in-plane displacements. The present paper presents the derivation of the nonlinear plate equations for buckling of plates loaded in axial compression for both higher order theories. This paper also presents postbuckling results for the average longitudinal compressive direct stress resultant and maximum stress resultants as a function of the applied displacements, and maximum out-of-plane displacement as a function of the applied displacement. The plates considered in this paper are long with side edges simply supported, free of normal stress, and free to slide along the edges to give constant strain. Results of the four theories are for aluminum plates loaded in uniaxial compressive end shortening.

Symbols

$A_{11}, A_{12}, A_{22}, A_{33}, A_{44}, A_{55}, A_{66}$	plate extensional stiffnesses
a, b, h	dimension of rectangular plate parallel to X, Y, and Z axis, respectively
$C_{11}, C_{12}, C_{22}, C_{33}, C_{44}, C_{55}, C_{66}$	stiffnesses used in Hooke's law

$D_{11}, D_{12}, D_{22}, D_{66}$	plate bending stiffnesses
E	Young's modulus
$H_{44}, I_{44}, J_{12}, J_{22}, J_{66}, K_{12}, K_{22}, K_{66}$	plate stiffness components
$L_x, L_y, L_z, L_{yz}, L_{xz}, L_{xy}, M_x, M_y, M_{xy}$	moment resultants in the plate
N_x, N_y, N_{xy}	in-plane stress resultants in the plate
N_{yz}, N_{xz}	transverse stress resultants in the plate
$N_{x,\mathrm{av}}$	average axial stress resultant
$N_{x,\mathrm{cr}}$	value of $N_{x,\mathrm{av}}$ at buckling
Q, Q_y	functions of y defined in appendix
U	applied end-shortening
u, v, w	displacement in x, y, and z direction, respectively
x, y, z	plate coordinates
β_1, β_2	functions of x and y defined in the appendix
$\epsilon_x, \epsilon_y, \epsilon_z, \gamma_{yz}, \gamma_{xz}, \gamma_{xy}$	strains in the plate
λ	buckle half-wavelength
μ	Poisson's ratio
$\sigma_x, \sigma_y, \sigma_z, \tau_{yz}, \tau_{xz}, \tau_{xy}$	stresses in the plate

Theory

A brief outline of the derivation of the four different theories compared in this paper is presented in this section. The derivation of equations using classical Kirchhoff theory has been presented in reference 5. The derivation of equations using first-order shear deformation theory has been presented in references 2 and 3. The two higher order theories are not given in detail elsewhere, so they are presented in the appendix. The general approach used in deriving the equations to be solved is the same as in reference 6. First, the displacement functions for each theory are identified. The nonlinear strain-displacement relations and the assumption that the displacements are sinusoidally periodic along the length of the infinitely long plate are incorporated. Stress-strain relations are defined for a "specially orthotropic" plate, and application of the principle of virtual work leads to ordinary differential equations and variationally consistent boundary conditions, which are solved by a computer program based on Newton's method.

The displacements considered for each theory are

Classical Kirchhoff theory:

$$\left.\begin{aligned} u(x,y,z) &= u^o(x,y) - w^o_{,x}(x,y)\frac{z}{h} \\ v(x,y,z) &= v^o(x,y) - w^o_{,y}(x,y)\frac{z}{h} \\ w(x,y,z) &= w^o(x,y) \end{aligned}\right\} \tag{1}$$

First-order shear deformation theory:

$$\left.\begin{aligned} u(x,y,z) &= u^o(x,y) + u^a(x,y)\frac{z}{h} \\ v(x,y,z) &= v^o(x,y) + v^a(x,y)\frac{z}{h} \\ w(x,y,z) &= w^o(x,y) \end{aligned}\right\} \tag{2}$$

Higher order shear deformation theory:

$$\left.\begin{aligned} u(x,y,z) &= u^o(x,y) + \left\{ u^a(x,y) - \frac{4h}{3}\left[\frac{u^a(x,y)}{h} + w^o_{,x}(x,y)\right]\left(\frac{z}{h}\right)^2 \right\}\frac{z}{h} \\ v(x,y,z) &= v^o(x,y) + \left\{ v^a(x,y) - \frac{4h}{3}\left[\frac{v^a(x,y)}{h} + w^o_{,y}(x,y)\right]\left(\frac{z}{h}\right)^2 \right\}\frac{z}{h} \\ w(x,y,z) &= w^o(x,y) \end{aligned}\right\} \tag{3}$$

Three-dimensional flexibility theory

$$\left.\begin{aligned} u(x,y,z) &= u^o(x,y) + u^a(x,y)\frac{z}{h} + u^s(x,y)\sin\frac{\pi z}{h} \\ v(x,y,z) &= v^o(x,y) + v^a(x,y)\frac{z}{h} + v^s(x,y)\sin\frac{\pi z}{h} \\ w(x,y,z) &= w^o(x,y) + w^c(x,y)\cos\frac{\pi z}{h} \end{aligned}\right\} \tag{4}$$

Both the classical Kirchhoff and the first-order shear deformation theories have in-plane deformations u and v which are linear in z. Classical theory, however, has the additional assumption that there is zero transverse shearing ($\gamma_{xz} = \gamma_{yz} = 0$), thus eliminating u^a and v^a in favor of derivatives of w^o.

Higher order shear deformation theory considers in-plane deformations u and v which are cubic in z. As explained in reference 6, the squared-in-z term vanishes and the cubic term does not introduce any new variables beyond those that appear in first-order shear deformation theory if the boundary conditions are satisfied at $z = \pm h/2$. The three-dimensional flexibility theory considers trigonometric terms in u, v, and w beyond the expressions considered for the deformations of first-order shear deformation theory. In this paper, the superscript o corresponds to the constant-in-z terms, the superscript a corresponds to the algebraic-in-z terms, and the superscripts s and c correspond to the trigonometric-in-z terms.

To account for the applied displacement U

$$\left.\begin{aligned} u^o(x,y) &= -U\frac{x}{a} + U_2^o(x,y) \\ v^o(x,y) &= v_0^o(y) + V_2^o(x,y) \end{aligned}\right\} \tag{5}$$

where numbered subscripts for loads, displacements, and curvatures indicate a y-dependence only. To satisfy the assumption that the displacements are sinusoidally periodic along the length x

$$\left.\begin{aligned} U_2^o &= u_2^o(y)\sin\frac{2\pi x}{\lambda} \\ V_2^o &= v_2^o(y)\cos\frac{2\pi x}{\lambda} \end{aligned}\right\} \tag{6}$$

All the other u coefficients can be expressed as functions of y multiplied by $\cos \pi x/\lambda$, where λ is the half-wavelength of the buckled plate. All the other v and w coefficients can be expressed as functions of y multiplied by $\sin \pi x/\lambda$. The strain-displacement relations used are

$$\left.\begin{aligned} \epsilon_x &= u_{,x} + \frac{1}{2}w_{,x}^2 \\ \epsilon_y &= v_{,y} + \frac{1}{2}w_{,y}^2 \\ \epsilon_z &= w_{,z} \\ \gamma_{yz} &= v_{,z} + w_{,y} \\ \gamma_{xz} &= u_{,z} + w_{,x} \\ \gamma_{xy} &= u_{,y} + v_{,x} + w_{,x}\, w_{,y} \end{aligned}\right\} \tag{7}$$

Hooke's law relating stresses to strains for a "specially orthotropic" material is used here

$$\begin{vmatrix} \sigma_x \\ \sigma_y \\ \sigma_z \\ \tau_{yz} \\ \tau_{xz} \\ \tau_{xy} \end{vmatrix} = \begin{bmatrix} C_{11} & C_{12} & 0 & 0 & 0 & 0 \\ C_{12} & C_{22} & 0 & 0 & 0 & 0 \\ 0 & 0 & C_{33} & 0 & 0 & 0 \\ 0 & 0 & 0 & C_{44} & 0 & 0 \\ 0 & 0 & 0 & 0 & C_{55} & 0 \\ 0 & 0 & 0 & 0 & 0 & C_{66} \end{bmatrix} \begin{vmatrix} \epsilon_x \\ \epsilon_y \\ \epsilon_z \\ \gamma_{yz} \\ \gamma_{xz} \\ \gamma_{xy} \end{vmatrix} \tag{8}$$

Ordinary differential equations and variationally consistent boundary conditions are derived using the principle of virtual work, and the equations are solved by Newton's method in a computer program discussed in reference 7. The principle of virtual work applied to the internal forces of a three-dimensional body considered here is

$$\delta \mathrm{II} = \int_0^a \int_0^b \int_{-h/2}^{h/2} (\sigma_x \delta\epsilon_x + \sigma_y\, \delta\epsilon_y + \sigma_z\, \delta\epsilon_z + \tau_{yz}\, \delta\gamma_{yz} + \tau_{xz}\, \delta\gamma_{xz} + \tau_{xy}\, \delta\gamma_{xy})\, dz\, dy\, dx \tag{9}$$

and the set of simple support boundary conditions at $y = 0$ and $y = b$ used are

$$\left.\begin{aligned} u &= U \\ N_y &= 0 \\ w &= 0 \\ M_y &= 0 \end{aligned}\right\} \tag{10}$$

The half-wavelength λ of the assumed deformations for the long plates considered is chosen to minimize the buckling load for each given applied deformation.

Results and Discussion

The results obtained in this study for aluminum plates with geometry as shown in figure 1 are based on the mechanical properties of Young's modulus $E = 10.7 \times 10^6$ psi and Poisson's ratio $\mu = 0.33$. Buckling results presented in figure 2 for an aluminum plate show the variation of buckling stress coefficient with width-to-thickness ratio b/h given by the four theories for a range of length-to-width ratio a/b. The differences in the buckling results for aluminum plates with width-to-thickness ratios less than 10 illustrate the need to include the effects of transverse shearing in determining the compressive buckling stress.

Characteristic curves for different values of b/h are presented in figure 3 for the postbuckling response of rectangular aluminum plates loaded in compression. For a b/h value of 100, only one curve is shown, since the corresponding results for each theory are approximately the same. For lower values of b/h, figure 3 shows that the normalized end-shortening U is larger for a shear deformable plate than for its infinitely rigid counterpart for a fixed value of normalized stress resultant $N_{x,\mathrm{av}}$. Present results indicate that three-dimensional flexibility theory gives lower buckling loads and therefore more accurate results. The shear deformation theory results are converged solutions for all values of b/h investigated, and this theory has the advantage of fewer unknowns than the three-dimensional theory. Results for the normalized stress resultants $N_{y,\max}$ and $N_{xy,\max}$, for different values of b/h, are presented in figures 4 and 5, respectively, and corresponding results for the normalized maximum deflection $w_{\max}$ are presented in figure 6. The results presented in figure 4 show that the higher order shear deformation theory gives the lowest value of normalized $N_{y,\max}$ for a given value of normalized end-shortening U. The results presented in figure 5 show that the normalized $N_{xy,\max}$ as a function of the normalized end-shortening U is nearly independent of the width-to-thickness ratio b/h for the cases investigated. Results for the normalized maximum deflection $w_{\max}$ show that the value of the deflection becomes increasingly dependent upon the width-to-thickness ratio b/h as the value of the normalized end-shortening U increases.

Detailed numerical results for the four theories for the range of b/h ratios investigated for the normalized end-shortening displacement parameter $\overline{U} = 14$ are presented in tables I through IV. The value of this applied displacement parameter equal to 14 is well into the postbuckling range. Results are presented in each table for the applied average in-plane stress resultant $\overline{N}_{x,\mathrm{av}}$, the maximum values of the other stress resultants, and the maximum transverse displacement. Table I shows that for $b/h = 100$, there is very little difference in the results given by the different theories. Table II indicates that as the b/h ratio decreases, that is, as the width of the plate narrows, small differences between the theoretical results occur. In tables III and IV, these differences become more pronounced, and although the three-dimensional flexibility theory does give more accurate results, the numerical procedure has difficulty converging for thicker plates. The omission of the first-order shear deformation theory results presented in tables III and IV and the omission of the three-dimensional flexibility theory results presented in table IV correspond to those values of b/h for which results were not obtained. An explanation for this inability to obtain results has not been determined.

The principle of virtual work requires only that the geometric boundary conditions be satisfied. The inclusion of additional terms in the representation of the through-the-thickness variation of the in-plane displacements will lead to convergence and the satisfaction of natural boundary conditions in the limit if a complete set of terms is used. An alternate approach is to use terms that satisfy the boundary conditions. A complete set of these terms also leads to convergence. For the present problem, the three-dimensional flexibility theory uses terms that do not satisfy the natural boundary conditions. In the higher order shear deformation theory, coefficients of u and v of the assumed displacements in equation (3) are chosen such that $\gamma_{xz} = 0$ and $\gamma_{yz} = 0$. The coefficients are written in terms of the existing unknowns u^a, v^a, and w^o in a form which satisfies the natural boundary conditions at the top and bottom surfaces of the plate. Comparisons of results are valid whether or not natural boundary conditions are satisfied.

Concluding Remarks

This paper presents buckling and postbuckling results for simply supported aluminum plates loaded in compression. The buckling results have been plotted to show the effects of varying plate width and thickness on the buckling stress coefficient. Buckling results are given for various plate length-to-width ratios. The buckling results for aluminum plates with width-to-thickness ratios less than 10 illustrate the need to include the effects of transverse shearing when determining the compressive buckling stress. Postbuckling results for plates with transverse shearing flexibility are compared with results from classical theory for various width-to-thickness ratios. The plates are considered to be long with side edges simply supported and stress free, and the plates are subjected to a longitudinal compressive end-shortening displacements. Characteristic curves indicating the average longitudinal direct stress resultant as a function of the applied displacements are calculated based on four different theories: classical Von Karman theory, first-order shear deformation theory, higher order shear deformation theory, and three-dimensional flexibility theory.

Present results indicate that the three-dimensional flexibility theory gives the lowest buckling loads for the four theories considered, and therefore the most accurate results. The higher order shear deformation theory has fewer unknowns to determine than the three-dimensional flexibility theory but is not as accurate. The figures presented

show that, for postbuckling, small differences occur in the average longitudinal direct stress resultant, in the maximum values of the other stress resultants, and in the maximum transverse displacements calculated when the effects of transverse shear flexibility are included in the various theories. Because of small differences in the results from the various theories, results are given in tables for the applied edge displacements into the postbuckling range. The principle of virtual work used in this study requires only that the geometric boundary conditions are satisfied. The most accurate results are obtained from the three-dimensional flexibility theory where enough terms are selected to satisfy the geometric boundary conditions but not the natural boundary conditions. In the higher order shear deformation theory, it is possible to select coefficients of the assumed displacements such that the transverse shear strains $\gamma_{xz} = 0$ and $\gamma_{yz} = 0$. These coefficients are written in terms of the existing unknown displacements u^1, v^a, and w^o in a form which satisfies the natural boundary conditions at the top and bottom surfaces of the plate. In this manner, results are obtained from the higher order shear deformation theory that are nearly as accurate as those obtained from the three-dimensional flexibility theory, but with considerably fewer unknowns.

NASA Langley Research Center
Hampton VA 23665-5225
May 25, 1990

Appendix

Derivation of the Governing Equations for the Higher Order Shear Deformation Theory and the Three-Dimensional Flexibility Theory

Governing differential equations are derived in more detail in this appendix for the two higher order theories considered in this paper.

Higher Order Shear Deformation Theory

The displacements used in this theory are given by equations (3) as

$$\left.\begin{aligned} u(x,y,z) &= u^o(x,y) + \left\{u^a(x,y) - \frac{4h}{3}\left[\frac{u^a(x,y)}{h} + w^o_{,x}(x,y)\right]\left(\frac{z}{h}\right)^2\right\}\frac{z}{h} \\ v(x,y,z) &= v^o(x,y) + \left\{v^a(x,y) - \frac{4h}{3}\left[\frac{v^a(x,y)}{h} + w^o_{,y}(x,y)\right]\left(\frac{z}{h}\right)^2\right\}\frac{z}{h} \\ w(x,y,z) &= w^o(x,y) \end{aligned}\right\} \tag{A1}$$

Substitution of equations (3) into equations (7) gives the strain-displacement relations

$$\left.\begin{aligned} \epsilon_x &= u^o_{,x} + \frac{1}{2}w^{o2}_{,x} + u^a_{,x}\frac{z}{h} - \frac{4}{3}\left(\frac{z}{h}\right)^3\left(u^a_{,x} + w^o_{,xx}\,h\right) \\ \epsilon_y &= v^o_{,y} + \frac{1}{2}w^{o2}_{,y} + v^a_{,y}\frac{z}{h} - \frac{4}{3}\left(\frac{z}{h}\right)^3\left(v^a_{,y} + w^o_{,yy}\,h\right) \\ \gamma_{xy} &= u^o_{,y} + v^o_{,x} + w^o_{,x}\,w^o_{,y} + \left(u^a_{,y} + v^a_{,x}\right)\frac{z}{h} - \frac{4}{3}\left(\frac{z}{h}\right)^3\left(u^a_{,y} + v^a_{,x} + 2w^o_{,xy}\,h\right) \\ \gamma_{xz} &= \left(w^o_{,x} + \frac{u^a}{h}\right)\left[1 - \left(\frac{2z}{h}\right)^2\right] \\ \gamma_{yz} &= \left(w^o_{,y} + \frac{v^a}{h}\right)\left[1 - \left(\frac{2z}{h}\right)^2\right] \end{aligned}\right\} \tag{A2}$$

The assumption of sinusoidal periodicity along the length leads to

$$\left.\begin{aligned} u^o &= -U\frac{x}{a} + u^o_2(y)\sin\frac{2\pi x}{\lambda} \\ u^a &= u^a_1(y)\cos\frac{\pi x}{\lambda} \\ w^o &= w^o_1(y)\sin\frac{\pi x}{\lambda} \\ v^o &= v^o_0(y) + v^o_2(y)\cos\frac{2\pi x}{\lambda} \\ v^a &= v^a_1(y)\sin\frac{\pi x}{\lambda} \end{aligned}\right\} \tag{A3}$$

Stresses are determined from Hooke's law according to equation (8), and stress resultant forces and moments are determined by the following integrals through the thickness

$$
\left.
\begin{aligned}
N_{x_0} + N_{x_2} \cos \frac{2\pi x}{\lambda} &= \int_{-h/2}^{h/2} \sigma_x \, dz \\
N_{y_0} + N_{y_2} \sin \frac{2\pi x}{\lambda} &= \int_{-h/2}^{h/2} \sigma_y \, dz \\
N_{yz_0} \sin \frac{\pi x}{\lambda} &= \int_{-h/2}^{h/2} \tau_{yz} \left(1 - \frac{4z^2}{h^2}\right) dz \\
N_{xz_0} \cos \frac{\pi x}{\lambda} &= \int_{-h/2}^{h/2} \tau_{xz} \left(1 - \frac{4z^2}{h^2}\right) dz \\
N_{xy_2} \sin \frac{2\pi x}{\lambda} &= \int_{-h/2}^{h/2} \tau_{xy} \, dz \\
M_{x_0} \sin \frac{\pi x}{\lambda} &= \int_{-h/2}^{h/2} \sigma_x z \, dz \\
M_{x_1} \sin \frac{\pi x}{\lambda} &= \int_{-h/2}^{h/2} -\frac{4}{3} h \sigma_x \left(\frac{z}{h}\right)^3 dz \\
M_{y_0} \sin \frac{\pi x}{\lambda} &= \int_{-h/2}^{h/2} \sigma_y z \, dz \\
M_{y_1} \sin \frac{\pi x}{\lambda} &= \int_{-h/2}^{h/2} -\frac{4}{3} h \sigma_y \left(\frac{z}{h}\right)^3 dz \\
M_{xy_0} \cos \frac{\pi x}{\lambda} &= \int_{-h/2}^{h/2} \tau_{xy} z \, dz \\
M_{xy_1} \cos \frac{\pi x}{\lambda} &= \int_{-h/2}^{h/2} -\frac{4}{3} h \tau_{xy} \left(\frac{z}{h}\right)^3 dz
\end{aligned}
\right\} \qquad \text{(A4)}
$$

Substitution of the stresses and strains into the virtual work expression, equation (9), and performing the variation leads to the differential equations

$$
\left.
\begin{aligned}
u_2^{o\prime} &= \frac{2\pi}{\lambda} v_2^o - \frac{1}{2} w_1^o \beta_2 \frac{\pi}{\lambda} + \frac{N_{xy_2}}{A_{66}} \\
v_2^{o\prime} &= \frac{1}{4}\beta_2^2 - \frac{A_{12}}{A_{22}} \left[u_2^o \frac{2\pi}{\lambda} + \frac{1}{4} w_1^{o2} \left(\frac{\pi}{\lambda}\right)^2 \right] + \frac{N_{y_2}}{A_{22}} \\
\frac{u_1^{a\prime}}{h} &= -\frac{v_{1\pi}^a}{h\lambda} + \left[M_{xy_1} - (\overline{D}_{66} + \overline{B}_{66}) \frac{2\pi}{\lambda} \beta_2 \right] \Big/ (D_{66} + 2\overline{D}_{66} + \overline{B}_{66}) \\
\frac{v_1^{a\prime}}{h} &= \left\{ \overline{B}_{22} (M_{y_o} - M_{y_1}) - \overline{D}_{22} M_{y_1} + (D_{12}\overline{B}_{22} - \overline{D}_{12}\overline{D}_{22}) \frac{u_{1\pi}^a}{h\lambda} \right. \\
&\qquad \left. + (\overline{D}_{12}\overline{B}_{22} - \overline{B}_{12}\overline{D}_{22}) \left[u_1^a \frac{\pi}{\lambda} + w_1^o \left(\frac{\pi}{\lambda}\right)^2 \right] \right\} \Big/ \left(D_{22}\overline{B}_{22} - \overline{D}_{22}^2 \right) \\
v_o^{o\prime} &= -\frac{1}{4}\beta_2^2 - \frac{A_{12}}{A_{22}} \left[-U + \frac{1}{4} w_1^{o2} \left(\frac{\pi}{\lambda}\right)^2 \right] + \frac{N_{y_o}}{A_{22}} \\
N'_{xy_2} &= \frac{2\pi}{\lambda} N_{x_2} \\
N'_{y_2} &= -\frac{2\pi}{\lambda} N_{xy_2} \\
M'_{xy_1} &= -\frac{\pi}{\lambda} (M_{x_0} + M_{x_1}) + A_{55} \left(\frac{u_1^a}{h} + w_1^o \frac{\pi}{\lambda} \right) \\
M'_{y_0} &= \frac{\pi}{\lambda} M_{xy_1} + A_{44} \left(\frac{v_1^a}{h} + \beta_2 \right) \\
N'_{y_0} &= 0 \\
Q'_y &= \left(\frac{\pi}{\lambda}\right)^2 \left(M_{x_0} + \frac{1}{2} M_{x_2} \right) w_1^o - M_{x_1} \left(\frac{\pi}{\lambda}\right)^2 + A_{55} \left(\frac{u_1^a}{h} + w_1^o \frac{\pi}{\lambda} \right) + \frac{1}{2} N_{xy_2} \beta_2 \frac{\pi}{\lambda} \\
M'_{y_1} &= \left(N_{y_0} - \frac{1}{2} N_{y_2} \right) \beta_2 + \frac{1}{2} N_{xy_2} w_1^o \frac{\pi}{\lambda} + \frac{2\pi}{\lambda} M_{xy_1} + A_{44} \left(\frac{v_1^a}{h} + \beta_2 \right) - Q_y
\end{aligned}
\right\} \tag{A5}
$$

The stiffnesses of the plate are given by

$$
\left.
\begin{aligned}
A_{ij} &= \int_{-h/2}^{h/2} C_{ij}\, dz \\
D_{ij} &= \int_{-h/2}^{h/2} C_{ij} z^2\, dz \\
\overline{B}_{ij} &= -\frac{D_{ij}}{21B^2} \cdot \text{in}^2 \\
\overline{D}_{ij} &= -\frac{D_{ij}}{5B} \cdot \text{in.}
\end{aligned}
\right\} \tag{A6}
$$

where the C_{ij} are the stiffnesses in equation (8). Using the definition $\beta_2 = w_1^{o\prime}$ gives the following two differential equations, which complete the set of equations (14 equations with 14 unknowns) without squares of derivatives of the unknowns:

$$\left.\begin{aligned} w_1^{o\prime} &= \beta_2 \\ \beta_2{}' &= -\frac{v_1^{a\prime}}{h} - \left\{ \overline{D}_{22}\left(M_{y_0} - M_{y_1}\right) - D_{22}M_{y_1} + \left(\overline{D}_{22}D_{12} - D_{22}\overline{D}_{12}\right)\frac{u_1^a}{h}\frac{\pi}{\lambda} \right. \\ &\quad \left. + \left(\overline{D}_{22}\overline{D}_{12} - D_{22}\overline{B}_{12}\right)\left[\frac{u_1^a}{h}\frac{\pi}{\lambda} + w_1^o\left(\frac{\pi}{\lambda}\right)^2\right] \right\} \Big/ \left(D_{22}\overline{B}_{22} - \overline{D}_{22}^2\right) \end{aligned}\right\} \tag{A7}$$

Squares of the derivatives are not retained in the computer program used.

The boundary conditions at $y = 0$ and $y = b$ that correspond to equations (10) are

$$\left.\begin{aligned} u_2^o = u_1^a &= 0 \\ N_{y_0} = N_{y_2} &= 0 \\ w_1^o &= 0 \\ M_{y_0} = M_{y_1} &= 0 \end{aligned}\right\} \tag{A8}$$

Three-Dimensional Flexibility Theory

The displacements used in this theory are given by equations (4) as

$$\left.\begin{aligned} u(x,y,z) &= u^o(x,y) + u^a(x,y)\frac{z}{h} + u^s(x,y)\sin\frac{\pi z}{h} \\ v(x,y,z) &= v^o(x,y) + v^a(x,y)\frac{z}{h} + v^s(x,y)\sin\frac{\pi z}{h} \\ w(x,y,z) &= w^o(x,y) + w^c(x,y)\cos\frac{\pi z}{h} \end{aligned}\right\} \tag{A9}$$

Substitution of equations (4) into equations (7) and neglecting the nonlinear terms involving w^c gives the strain-displacement relations

$$\left.\begin{aligned} \epsilon_x &= u_{,x}^o + \frac{1}{2}w_{,x}^{o2} + u_{,x}^a\frac{z}{h} + u_{,x}^s\sin\frac{\pi z}{h} \\ \epsilon_y &= v_{,y}^o + \frac{1}{2}w_{,y}^{o2} + v_{,y}^a\frac{z}{h} + v_{,y}^s\sin\frac{\pi z}{h} \\ \epsilon_z &= -\frac{\pi}{h}w^c\sin\frac{\pi z}{h} \\ \gamma_{xy} &= u_{,y}^o + v_{,x}^o + w_{,x}^o w_{,y}^o + \left(u_{,y}^a + v_{,x}^a\right)\frac{z}{h} + \left(u_{,y}^s + v_{,x}^s\right)\sin\frac{\pi z}{h} \\ \gamma_{xz} &= w_{,x}^o + \frac{u^a}{h} + \left(w_{,x}^c + \frac{\pi}{h}u^s\right)\cos\frac{\pi z}{h} \\ \gamma_{yz} &= \frac{v^a}{h} + w_{,y}^o + \left(\frac{\pi}{h}v^s + w_{,y}^c\right)\cos\frac{\pi z}{h} \end{aligned}\right\} \tag{A10}$$

The assumption of sinusoidal periodicity along the length leads to

$$\left.\begin{aligned} u^o &= -U\frac{x}{a} + u_2^o(y)\sin\frac{2\pi x}{\lambda} \\ u^a &= u_1^a(y)\cos\frac{\pi x}{\lambda} \\ u^s &= u_1^s(y)\cos\frac{\pi x}{\lambda} \\ v^o &= v_0^o(y) + v_2^o(y)\cos\frac{2\pi x}{\lambda} \\ v^a &= v_1^a(y)\sin\frac{\pi x}{\lambda} \\ v^s &= v_1^s(y)\sin\frac{\pi x}{\lambda} \\ w^o &= w_1^o(y)\sin\frac{\pi x}{\lambda} \\ w^c &= w_1^c(y)\sin\frac{\pi x}{\lambda} \end{aligned}\right\} \tag{A11}$$

Stresses are determined from Hooke's law according to equation (8), and stress resultant forces and moments are determined by the following integrals through the thickness

$$\left.\begin{aligned} N_{x_0} + N_{x_2}\cos\frac{2\pi x}{\lambda} &= \int_{-h/2}^{h/2}\sigma_x^o\,dz & M_{xy_1} &= \int_{-h/2}^{h/2}\left[\tau_{xy}^a\left(\frac{z}{h}\right) + \tau_{xy}^s\sin\frac{\pi z}{h}\right]\frac{z}{h}\,dz \\ N_{y_2}\sin\frac{2\pi x}{\lambda} &= \int_{-h/2}^{h/2}\sigma_y^o\,dz & L_{x_1} &= \int_{-h/2}^{h/2}\left[\sigma_x^a\left(\frac{z}{h}\right) + \sigma_x^s\sin\frac{\pi z}{h}\right]\sin\frac{\pi z}{h}\,dz \\ N_{yz_1} &= \int_{-h/2}^{h/2}\tau_{yz}^o\,dz & L_{y_1} &= \int_{-h/2}^{h/2}\left[\sigma_y^a\left(\frac{z}{h}\right) + \sigma_y^s\sin\frac{\pi z}{h}\right]\sin\frac{\pi z}{h}\,dz \\ N_{xz_1} &= \int_{-h/2}^{h/2}\tau_{xz}^o\,dz & L_{z_1} &= \int_{-h/2}^{h/2}\sigma_z^s\sin^2\frac{\pi z}{h}\,dz \\ N_{xy_2}\sin\frac{2\pi x}{\lambda} &= \int_{-h/2}^{h/2}\tau_{xy}^o\,dz & L_{yz_1} &= \int_{-h/2}^{h/2}\tau_{yz}^c\cos^2\frac{\pi z}{h}\,dz \\ M_{x_1} &= \int_{-h/2}^{h/2}\left[\sigma_x^a\left(\frac{z}{h}\right) + \sigma_x^s\sin\frac{\pi z}{h}\right]\frac{z}{h}\,dz & L_{xz_1} &= \int_{-h/2}^{h/2}\tau_{xz}^c\cos^2\frac{\pi z}{h}\,dz \\ M_{y_1} &= \int_{-h/2}^{h/2}\left[\sigma_y^a\left(\frac{z}{h}\right) + \sigma_y^s\sin\frac{\pi z}{h}\right]\frac{z}{h}\,dz & L_{xy_1} &= \int_{-h/2}^{h/2}\left[\tau_{xy}^a\left(\frac{z}{h}\right) + \tau_{xy}^s\sin\frac{\pi z}{h}\right]\sin\frac{\pi z}{h}\,dz \end{aligned}\right\} \tag{A12}$$

Substitution of the stresses and strains into the virtual work expression, equation (9), and performing the variation leads to the differential equations

$$
\left.
\begin{aligned}
u_2^{o\prime} &= \frac{2\pi}{\lambda} v_2^o - \frac{1}{2} w_1^o \beta_1 \frac{\pi}{\lambda} + \frac{N_{xy_2}}{A_{66}} \\
v_2^{o\prime} &= \frac{1}{4}\beta_1^2 - \frac{A_{12}}{A_{22}}\left[u_2^o \frac{2\pi}{\lambda} + \frac{1}{4} w_1^{o2} \left(\frac{\pi}{\lambda}\right)^2\right] + \frac{N_{y_2}}{A_{22}} \\
\frac{u_1^{a\prime}}{h} &= -\frac{v_1^a}{h}\frac{\pi}{\lambda} + \left(M_{xy_1} - \frac{J_{66}}{K_{66}} L_{xy_1}\right) \Big/ \left(D_{66} - \frac{J_{66}^2}{K_{66}}\right) \\
\frac{v_1^{a\prime}}{h} &= \left[\frac{L_{y_1}}{K_{22}} - \frac{M_{y_1}}{J_{22}} + \left(\frac{J_{12}}{K_{22}} - \frac{D_{12}}{J_{22}}\right)\frac{u_1^a}{h}\frac{\pi}{\lambda} + \left(\frac{K_{12}}{K_{22}} - \frac{J_{12}}{J_{22}}\right) u_1^s \frac{\pi}{\lambda}\right] \Big/ \left(\frac{J_{22}}{K_{22}} - \frac{D_{22}}{J_{22}}\right) \\
u_1^{s\prime} &= -\frac{\pi}{\lambda} v_1^s + \left(\frac{L_{xy_1}}{J_{66}} - \frac{M_{xy_1}}{D_{66}}\right) \Big/ \left(\frac{K_{66}}{J_{66}} - \frac{J_{66}}{D_{66}}\right) \\
v_1^{s\prime} &= \left[\frac{L_{y_1}}{J_{22}} - \frac{M_{y_1}}{D_{22}} + \left(\frac{J_{12}}{J_{22}} - \frac{D_{12}}{D_{22}}\right)\frac{u_1^a}{h}\frac{\pi}{\lambda} + \left(\frac{K_{12}}{J_{22}} - \frac{J_{12}}{D_{22}}\right) u_1^s \frac{\pi}{\lambda}\right] \Big/ \left(\frac{K_{22}}{J_{22}} - \frac{J_{22}}{D_{22}}\right) \\
w_1^{o\prime} &= -\frac{v_1^a}{h} + \left(\frac{N_{yz_1}}{H_{44}} - \frac{L_{yz_1}}{I_{44}}\right) \Big/ \left(\frac{A_{44}}{H_{44}} - \frac{H_{44}}{I_{44}}\right) \\
w_1^{c\prime} &= -\frac{\pi}{h} v_1^s - \left(\frac{N_{yz_1}}{A_{44}} - \frac{L_{yz_1}}{H_{44}}\right) \Big/ \left(\frac{I_{44}}{H_{44}} - \frac{H_{44}}{A_{44}}\right)
\end{aligned}
\right\} \qquad \text{(A13)}
$$

$$
\left.
\begin{aligned}
N_{xy_2}{}' &= \frac{2\pi}{\lambda} N_{x_2} \\
N_{y_2}{}' &= -\frac{2\pi}{\lambda} N_{xy_2} \\
M_{xy_1}{}' &= N_{xz_1} - M_{x_1}\frac{\pi}{\lambda} \\
M_{y_1}{}' &= N_{yz_1} + M_{xy_1}\frac{\pi}{\lambda} \\
L_{xy_1}{}' &= L_{xz_1}\frac{\pi}{h} - L_{x_1}\frac{\pi}{\lambda} \\
L_{yz_1}{}' &= L_{xz_1}\frac{\pi}{\lambda} - L_{z_1}\frac{\pi}{h} \\
L_{y_1}{}' &= L_{yz_1}\frac{\pi}{h} + L_{xy_1}\frac{\pi}{\lambda} \\
Q' &= \left(N_{x_0}^o + \frac{N_{x_2}}{2}\right) w_1^o \left(\frac{\pi}{\lambda}\right)^2 + \frac{1}{2} N_{xy_2}\beta_1 \frac{\pi}{\lambda} + N_{xz_1}\frac{\pi}{\lambda}
\end{aligned}
\right\}
$$

The stiffnesses of the plate are given by

$$\left.\begin{aligned} A_{ij} &= \int_{-h/2}^{h/2} C_{ij}\, dz \\ D_{ij} &= \int_{-h/2}^{h/2} C_{ij} z^2\, dz \\ H_{ij} &= \int_{-h/2}^{h/2} C_{ij} \cos\frac{\pi z}{h}\, dz \\ J_{ij} &= \int_{-h/2}^{h/2} C_{ij} z \sin\frac{\pi z}{h}\, dz \\ K_{ij} &= \int_{-h/2}^{h/2} C_{ij} \sin^2\frac{\pi z}{h}\, dz \\ I_{ij} &= \int_{-h/2}^{h/2} C_{ij} \cos^2\frac{\pi z}{h}\, dz \end{aligned}\right\} \tag{A14}$$

where the C_{ij} are the stiffnesses in equation (8). The definition $\beta_1 = w_1^{o\prime}$ is not used in this theory because of the difference in the unknowns in the theories. Instead, the following definition of β_1 is used

$$\beta_1 = \left\{ -\frac{v_1^a}{h} + \left[\frac{1}{H_{44}} \left(Q - \frac{1}{2}\frac{\pi}{\lambda} N_{xy_2} w_1^o \right) - \frac{L_{yz_1}}{I_{44}} \right] \Bigg/ \left(\frac{A_{44}}{H_{44}} - \frac{H_{44}}{I_{44}} \right) \right\} \Bigg/ \left[1 + \frac{N_{y_2}}{2H_{44}} \Bigg/ \left(\frac{A_{44}}{H_{44}} - \frac{H_{44}}{I_{44}} \right) \right] \tag{A15}$$

which results in the completely defined set of equations (16 equations with 16 unknowns) without squares of derivatives of the unknowns, which are not retained in the computer program used.

The boundary conditions used at $y = 0$ and $y = b$ that correspond to equation (10) are

$$\left.\begin{aligned} u_2^o = u_1^a = u_1^s &= 0 \\ N_{y_0} = N_{y_2} &= 0 \\ w_1^o = w_1^c &= 0 \\ M_{y_1} = L_{y_1} &= 0 \end{aligned}\right\} \tag{A16}$$

References

1. Stein, Manuel: Nonlinear Theory for Plates and Shells Including the Effects of Transverse Shearing. *AIAA J.*, vol. 24, no. 9, Sept. 1986, pp. 1537–1544.
2. Stein, Manuel; and Bains, Nancy Jane C.: Postbuckling Behavior of Longitudinally Compressed Orthotropic Plates With Three-Dimensional Flexibility. AIAA-86-0976, May 1986.
3. Stein, Manuel: Postbuckling of Orthotropic Composite Plates Loaded in Compression. *AIAA J.*, vol. 21, no. 12, Dec. 1983, pp. 1729–1735.
4. Mindlin, R. D.: Influence of Rotatory Inertia and Shear on Flexural Motions of Isotropic, Elastic Plates. *J. Appl. Mech.*, vol. 18, no. 1, Mar. 1951, pp. 31–38.
5. Librescu, L.; and Stein, M.: A Geometrically Nonlinear Theory of Shear Deformable Laminated Composite Plates and Its Use in the Postbuckling Analysis. *ICAS Proceedings 1988 – 16th Congress of the International Council of the Aeronautical Sciences*, 1988, pp. 349–359. (Available as ICAS-88-5.2.4.)
6. Reissner, Eric: The Effect of Transverse Shear Deformation on the Bending of Elastic Plates. *J. Applied Mech.*, vol. 12, no. 2, June 1945, pp. A-69–A-77.
7. Lentini, M.; and Pereyra, V.: An Adaptive Finite Difference Solver for Nonlinear Two-Point Boundary Problems with Mild Boundary Layers. *SIAM J. Numer. Anal.*, vol. 14, no. 1, Mar. 1977, pp. 91–111.

Table I. Stress Resultants and Transverse Displacement for $b/h = 100$ at $^{\dagger}\overline{U} = 14$

Theory	$\overline{N}_{x,\mathrm{av}}$	$\overline{N}_{y,\max}$	$\overline{N}_{xy,\max}$	$w_{\max}/h$
Classical	7.63970	2.69335	1.95480	0.15466
First-order shear deformation	7.65298	2.70474	1.95260	.15465
Higher order shear deformation	7.65165	2.73821	1.97692	.15571
Three-dimensional flexibility	7.61673	2.67665	1.96602	.15468

† Barred quantities are nondimensional quantities given by

$$\overline{U} = \frac{U(A_{11} - A_{12}^2/A_{22})b^2}{a\sqrt{D_{11}D_{22}}\,\pi^2} \quad \overline{N}_{x,\mathrm{av}} = \frac{N_{x,\mathrm{av}}\,b^2}{\sqrt{D_{11}D_{22}}\,\pi^2} \quad \overline{N}_{y,\max} = \frac{N_{y,\max}\,b^2}{\sqrt{D_{11}D_{22}}\,\pi^2} \quad \overline{N}_{xy,\max} = \frac{N_{xy,\max}\,b^2}{\sqrt{D_{11}D_{22}}\,\pi^2}$$

Table II. Stress Resultants and Transverse Displacement for $b/h = 20$ at $^{\dagger}\overline{U} = 14$

Theory	$\overline{N}_{x,\mathrm{av}}$	$\overline{N}_{y,\max}$	$\overline{N}_{xy,\max}$	$w_{\max}/h$
Classical	7.63970	2.69335	1.95480	0.15466
First-order shear deformation	7.55385	2.65594	1.97912	.15416
Higher order shear deformation	7.60060	2.64025	1.92883	.15255
Three-dimensional flexibility	7.51680	2.68240	1.97278	.15389

† Barred quantities are nondimensional quantities given by

$$\overline{U} = \frac{U(A_{11} - A_{12}^2/A_{22})b^2}{a\sqrt{D_{11}D_{22}}\,\pi^2} \quad \overline{N}_{x,\mathrm{av}} = \frac{N_{x,\mathrm{av}}\,b^2}{\sqrt{D_{11}D_{22}}\,\pi^2} \quad \overline{N}_{y,\max} = \frac{N_{y,\max}\,b^2}{\sqrt{D_{11}D_{22}}\,\pi^2} \quad \overline{N}_{xy,\max} = \frac{N_{xy,\max}\,b^2}{\sqrt{D_{11}D_{22}}\,\pi^2}$$

Table III. Stress Resultants and Transverse Displacement for $b/h = 10$ at $^{\dagger}\overline{U} = 14$

Theory	$\overline{N}_{x,\mathrm{av}}$	$\overline{N}_{y,\max}$	$\overline{N}_{xy,\max}$	$w_{\max}/h$
Classical	7.63970	2.69335	1.95480	0.15466
Higher order shear deformation	7.37103	2.53324	1.92198	.15039
Three-dimensional flexibility	7.20968	2.70648	1.99174	.15011

† Barred quantities are nondimensional quantities given by

$$\overline{U} = \frac{U(A_{11} - A_{12}^2/A_{22})b^2}{a\sqrt{D_{11}D_{22}}\,\pi^2} \quad \overline{N}_{x,\mathrm{av}} = \frac{N_{x,\mathrm{av}}\,b^2}{\sqrt{D_{11}D_{22}}\,\pi^2} \quad \overline{N}_{y,\max} = \frac{N_{y,\max}\,b^2}{\sqrt{D_{11}D_{22}}\,\pi^2} \quad \overline{N}_{xy,\max} = \frac{N_{xy,\max}\,b^2}{\sqrt{D_{11}D_{22}}\,\pi^2}$$

Table IV. Stress Resultants and Transverse Displacement for $b/h = 5$ at $^{\dagger}\overline{U} = 14$

Theory	$\overline{N}_{x,\mathrm{av}}$	$\overline{N}_{y,\max}$	$\overline{N}_{xy,\max}$	$w_{\max}/h$
Classical	7.63970	2.69335	1.95480	0.15466
Higher order shear deformation	7.26598	2.48961	1.97121	.14796

† Barred quantities are nondimensional quantities given by

$$\overline{U} = \frac{U(A_{11} - A_{12}^2/A_{22})b^2}{a\sqrt{D_{11}D_{22}}\,\pi^2} \quad \overline{N}_{x,\mathrm{av}} = \frac{N_{x,\mathrm{av}}\,b^2}{\sqrt{D_{11}D_{22}}\,\pi^2} \quad \overline{N}_{y,\max} = \frac{N_{y,\max}\,b^2}{\sqrt{D_{11}D_{22}}\,\pi^2} \quad \overline{N}_{xy,\max} = \frac{N_{xy,\max}\,b^2}{\sqrt{D_{11}D_{22}}\,\pi^2}$$

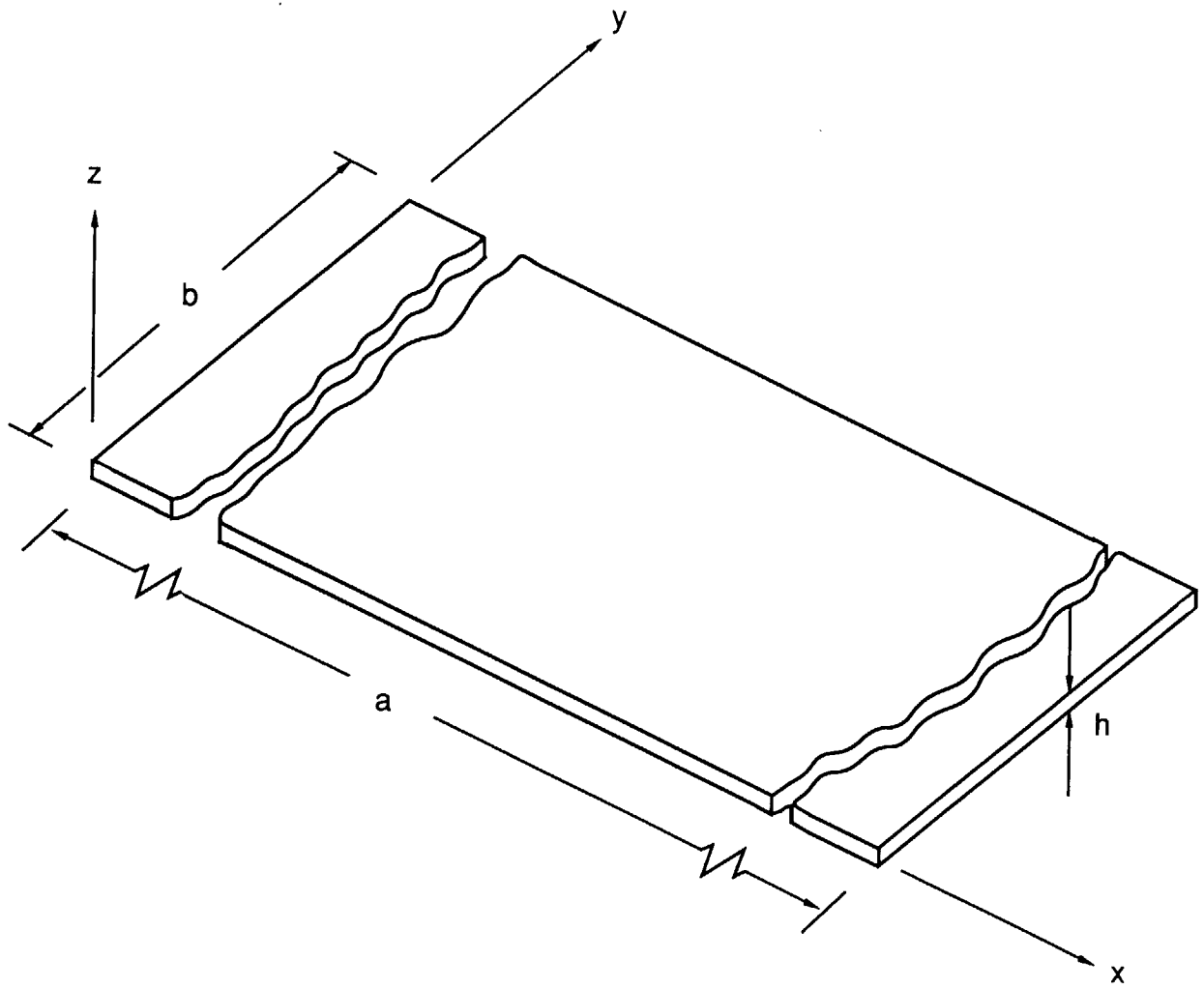

Figure 1. Plate geometry.

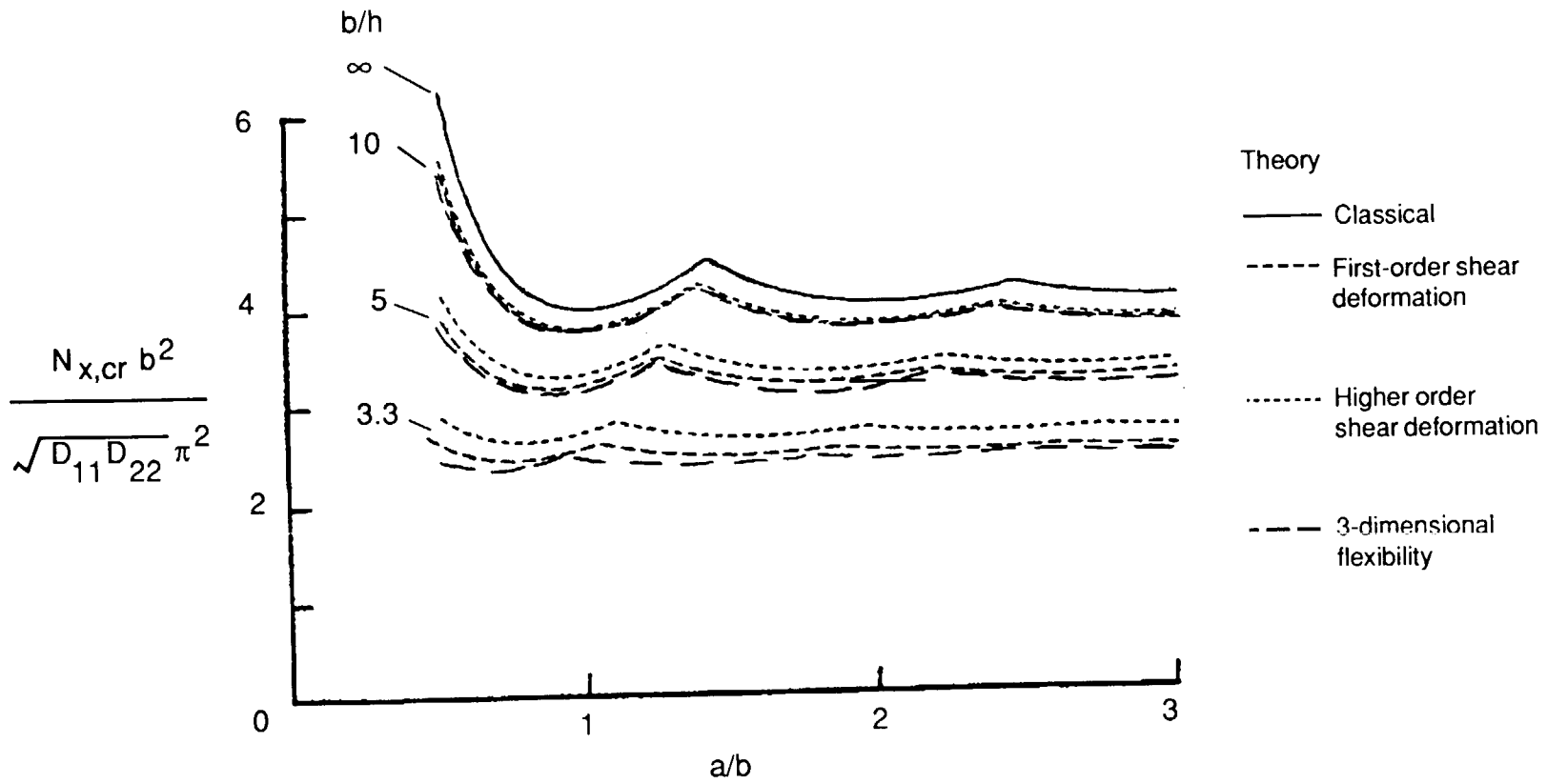

Figure 2. Critical axial stress resultant $N_{x,\mathrm{cr}}$ versus plate length-to-width ratio a/b for different width-to-thickness ratios b/h and different theories for aluminum plates of finite length.

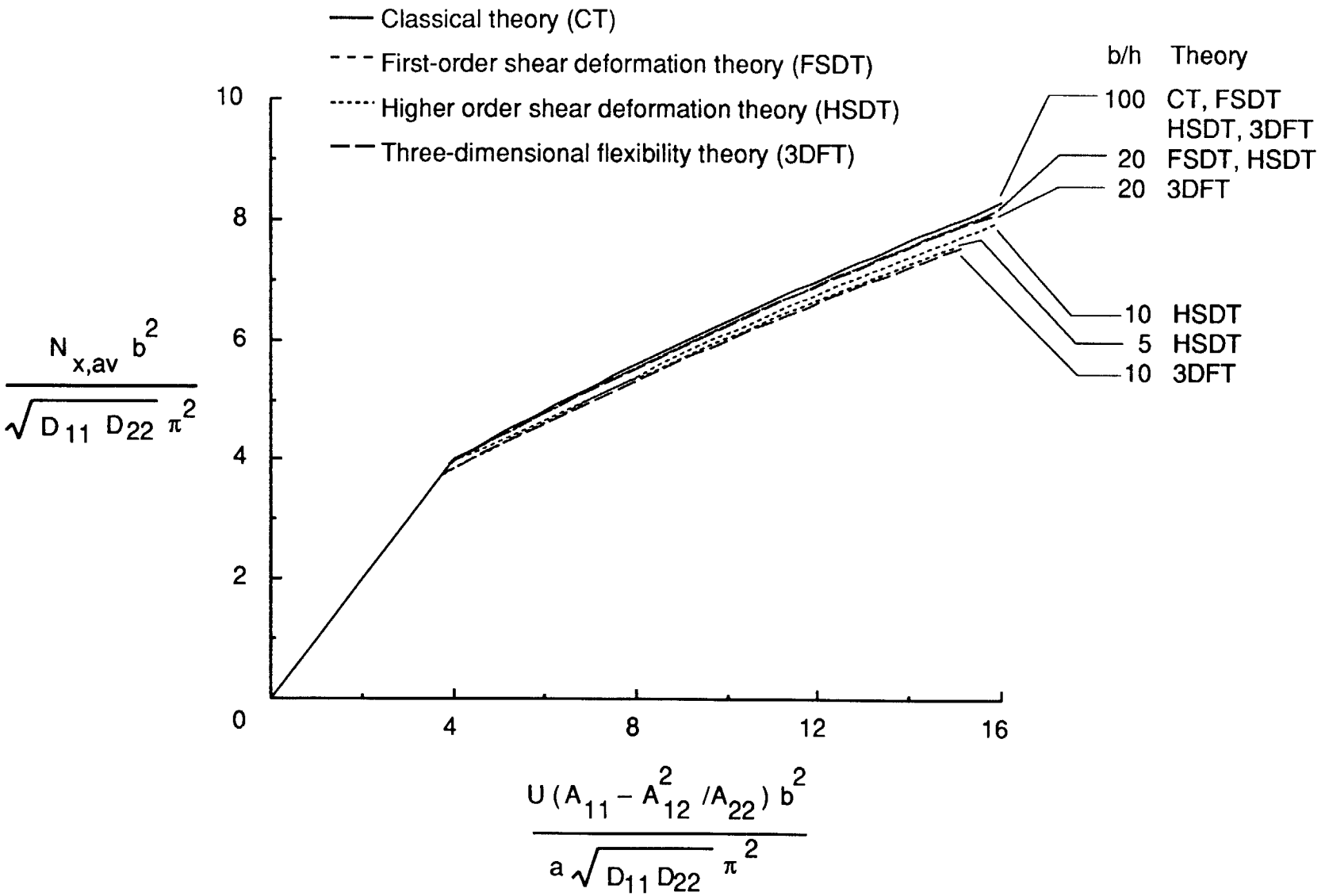

Figure 3. Average axial stress resultant $N_{x,\mathrm{av}}$ versus applied end-shortening U for different width-to-thickness ratios b/h and different theories for aluminum plates of infinite length where U/a is finite.

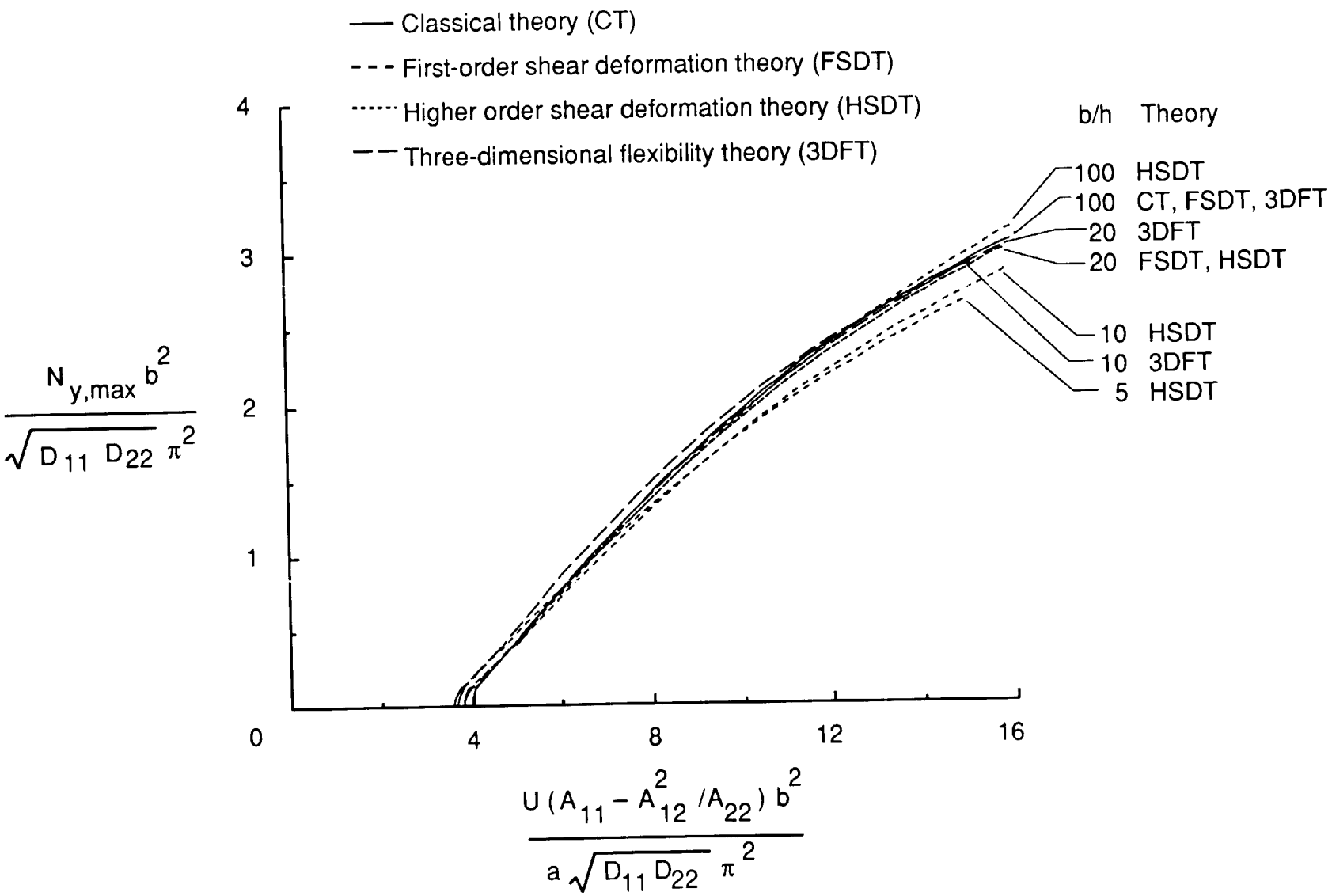

Figure 4. Maximum transverse stress resultant $N_{y,\max}$ versus applied end-shortening U for different width-to-thickness ratios b/h and different theories for aluminum plates of infinite length where U/a is finite.

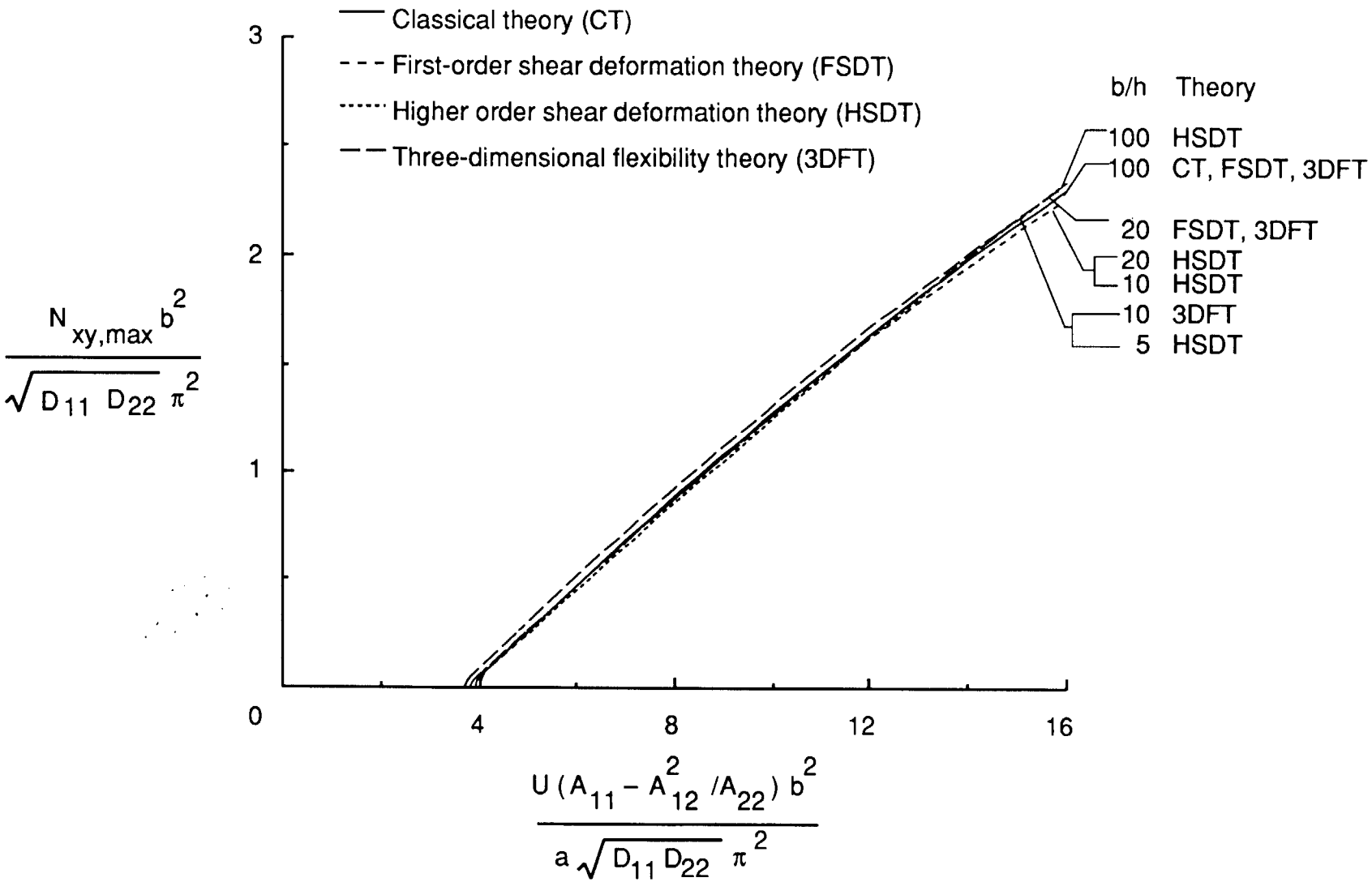

Figure 5. Maximum shear stress resultant $N_{xy,\max}$ versus applied end-shortening U for different width-to-thickness ratios b/h and different theories for aluminum plates of infinite length where U/a is finite.

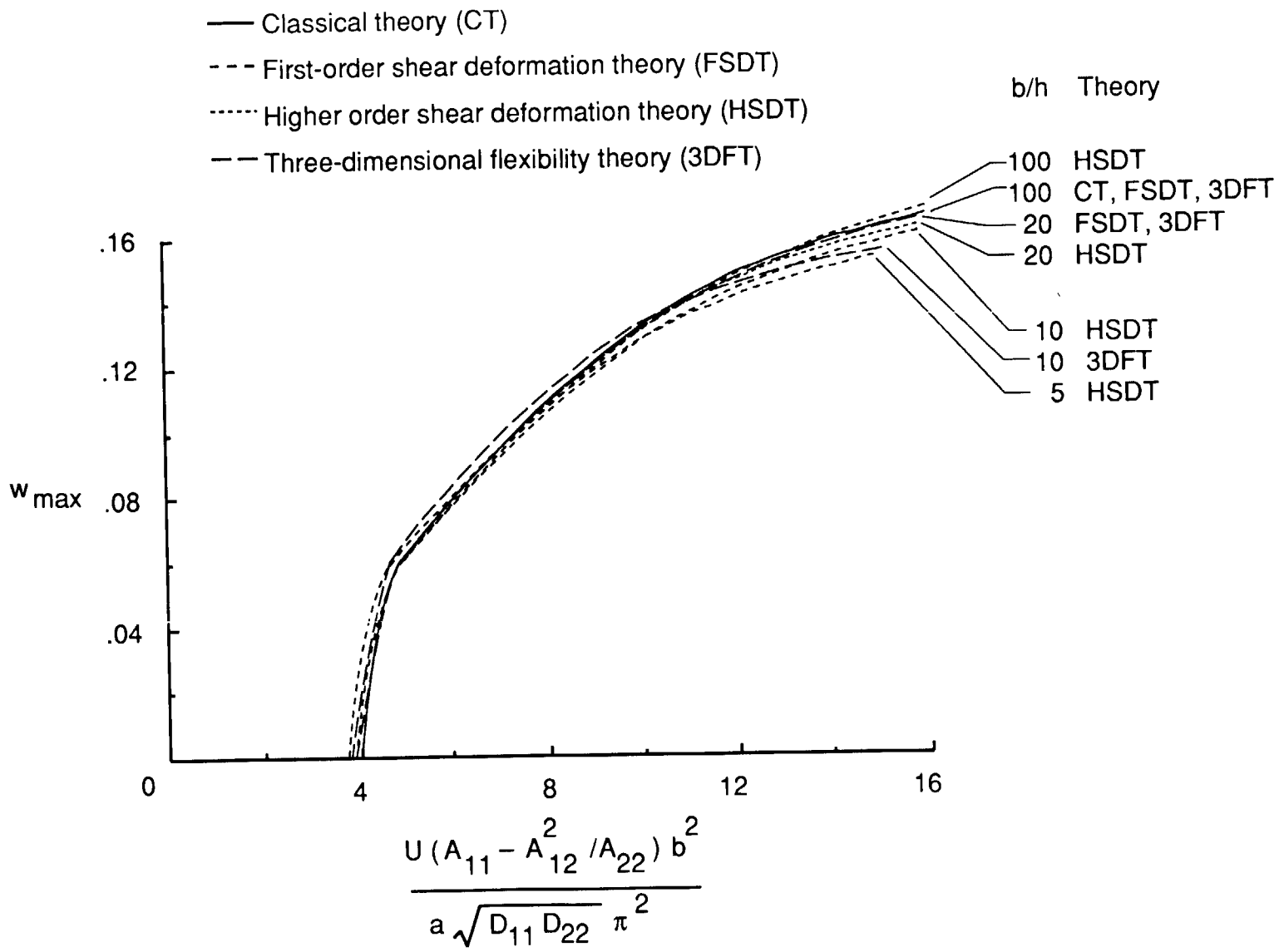

Figure 6. Maximum out-of-plane displacement $w_{\max}$ versus applied end-shortening U for different width-to-thickness ratios b/h and different theories for aluminum plates of infinite length where U/a is finite.

NASA
National Aeronautics and Space Administration

Report Documentation Page

1. Report No.	2. Government Accession No.	3. Recipient's Catalog No.
NASA TM-4199		

4. Title and Subtitle	5. Report Date
Postbuckling Response of Long Thick Isotropic Plates Loaded in Compression Including Higher Order Transverse Shearing Effects	September 1990
	6. Performing Organization Code
7. Author(s)	8. Performing Organization Report No.
Manuel Stein, P. Daniel Sydow, and Liviu Librescu	L-16756
9. Performing Organization Name and Address	10. Work Unit No.
NASA Langley Research Center Hampton, VA 23665–5225	505-63-01-09
	11. Contract or Grant No.
12. Sponsoring Agency Name and Address	13. Type of Report and Period Covered
National Aeronautics and Space Administration Washington, DC 20546–0001	Technical Memorandum
	14. Sponsoring Agency Code

15. Supplementary Notes

Manuel Stein and P. Daniel Sydow: Langley Research Center, Hampton, Virginia.
Liviu Librescu: Virginia Polytechnic Institute and State University, Blacksburg, Virginia.
Presented at Third ASCE/ASME Joint Mechanics Conference, July 9–12, 1989, San Diego, California.

16. Abstract

This paper presents buckling and postbuckling results for simply supported aluminum plates loaded in compression. Buckling results have been plotted to show the effects of thickness on the buckling stress coefficient. Buckling results are given for various length-to-width ratios. Postbuckling results for plates with transverse shearing flexibility are compared with results from classical theory for various width-to-thickness ratios. The plates are considered to be long with side edges simply supported and free of stress. The plates are subjected to a longitudinal compressive end-shortening displacement. Characteristic curves indicating the average longitudinal direct stress resultant as a function of the applied displacements are calculated based on four different theories: classical Von Karman theory, first-order shear deformation theory, higher order shear deformation theory, and three-dimensional flexibility theory. Present results indicate that the three-dimensional flexibility theory gives the lowest buckling loads and, therefore, the most accurate results. The higher order shear deformation theory has fewer unknowns than the three-dimensional flexibility theory but is not as accurate. The figures presented show that for postbuckling small differences occur in the average longitudinal direct stress resultant, in the maximum values of the transverse stress resultant and shear stress resultant, and in the maximum transverse displacements calculated when the effects of transverse shear flexibility are included in the various theories.

17. Key Words (Suggested by Authors(s))	18. Distribution Statement
Postbuckling analysis Rectangular plates Isotropic plates Compression loading	Unclassified—Unlimited Subject Category 39

19. Security Classif. (of this report)	20. Security Classif. (of this page)	21. No. of Pages	22. Price
Unclassified	Unclassified	22	A03

NASA FORM 1626 OCT 86

NASA-Langley, 1990

For sale by the National Technical Information Service, Springfield, Virginia 22161-2171